Poly(propylene oxide)−Poly(phenylene ethynylene) Block and Graft Copolymers

Marco A. Balbo Block[†] and Stefan Hecht[*,‡,†]

Department of Chemistry, Humboldt-Universität zu Berlin, 12489 Berlin, Germany, and the Max-Planck-Institut für Kohlenforschung, 45470 Mülheim an der Ruhr, Germany

Received December 21, 2007; Revised Manuscript Received February 17, 2008

ABSTRACT: Block copolymers composed of a highly isotactic and nonracemic poly(propylene oxide) (PPO) segment joined to a poly(phenylene ethynylene) (PPE) segment, with either *meta* or *para* connectivity, were synthesized, and their aggregation and conformational behavior in solution properties was investigated by optical spectroscopy. Furthermore, graft copolymers based on a *m*-phenylene ethynylene backbone equipped with isotactic, nonracemic PPO side chains were synthesized and studied with regard to their backbone conformation in solution. The combination of flexible chiral polymeric segments (PPO) with rather rigid, extended aromatic segments (PPE) promises to be a fruitful concept for generating novel optoelectronic materials with defined levels of intra- and intermolecular organization, i.e., backbone conformation and self-assembly behavior.

Introduction

Meshing characteristics of different homopolymers into a single block copolymer architecture is not comparable to the mere blending of the individual homopolymer components and grants access to unique properties, not found in either homopolymer, that arise from the possibility of chain segregation.[1] Phase separation leads to the generation of manifold morphologies in the bulk and at interfaces tunable by frequently competing interactions between the different segments[2] and thus provides an attractive nonlithographic "bottom-up" route to nanostructures.[3] Depending on the flexibility of the segments, coil−coil and rod−coil block copolymers are distinguished, the latter possessing a rigid and hardly flexible rodlike segment. While the assembly characteristics of coil−coil block copolymers are mainly governed by phase separation, in rod−coil block copolymers selective aggregation with high structural order or even crystallization of the rodlike segments usually dominates self-assembly[2b] while the flexible coil predominantly serves to separate the ordered phases. Of particular interest are copolymers containing π-conjugated segments. Processability of conjugated polymers often suffers from poor solubility due to the polymers' strong aggregation tendency caused by the inherent stiffness and therefore low flexibility of the extended aromatic backbones. Aggregation in solution and crystallization in films dramatically affects the optical and electronic properties of the materials, as interchain contacts alter absorption characteristics, quench emission, and impact conduction behavior. In recent years, block copolymer architectures have been successfully used to control the orientation of π-conjugated moieties and morphology of the resulting optically and electronically active, yet processable materials.[4] The role of the flexible segments in such block copolymers primarily is to increase overall solubility, thereby "diluting" the functional π-conjugated segments and reducing intermolecular contacts and aggregation. While these hybrid materials exhibit great potential for (opto)-electronic applications, it would be desirable to introduce chirality as another important feature to control aggregation.[5] Chirality has proven as an important factor in the self-assembly of π-conjugated materials[6] as well as the conformational behavior of helical polymers.[7] However, chirality usually originates from one chiral center in close proximity to the conjugated segments and monomer units. Here, we describe our efforts to utilize flexible, chiral, i.e., nonracemic and therefore enantiomerically pure, poly(propylene oxide) (PPO) blocks to affect aggregation and folding of *para*- and *meta*-connected poly(phenylene ethynylene)s (P*p*PE and P*m*PE, respectively) in solution.

Results and Discussion

Poly(propylene oxide) Blocks. Our approach is based on highly isotactic and nonracemic PPO, obtained by polymerization of enantiomerically pure (*S*)-propylene oxide (PO), as the flexible coil block and unsubstituted P*p*PE and P*m*PE as the rigid and folding rod blocks, respectively. The use of nonracemic PPO facilitates purification due to the feasibility of recrystallization from acetone and enables the possibility of chirality transfer from the PPO block to the P*p*PE or P*m*PE segment to affect aggregation and folding, respectively, while allowing convenient monitoring of these processes by CD spectroscopy. The copolymer synthesis starts from carefully prepared PPO segments of controlled lengths and low polydispersities (vide infra). Anchoring of a suitable entity, i.e., aromatic halide or acetylene, onto the PPOs' single terminal hydroxyl groups activates the PPO segments for subsequent Sonogashira−Hagihara cross-couplings. Thus, the second P*p*PE or P*m*PE blocks will be directly joined to the activated PPO block by applying a large excess of monomer,[8] a procedure resembling synthetic soluble support methodologies.[9] This approach not only promises a rapid access to such block copolymers but also is crucial for generating longer PPE segments, as preformed rod segments without solubilizing side chains are severely prone to aggregation and precipitation, precluding their synthetic accessibility. The concurrent homopolymerization of PE monomers in solution resembles a drawback of the approach as considerable amounts of monomer are wasted; however, this undesired side reaction should not hamper block copolymer formation and isolation, as longer homopolymers lacking solubilizing side chains will precipitate from the reaction mixture and shorter, still soluble PE oligomers will remain in solution during selective precipitation of the PPO-containing block copolymers.

Synthesis. The synthetic procedure for poly(propylene oxide)s was adopted from the work of Deffieux and co-workers.[10] Benzyl alkoxide **1**, generated by deprotonation of benzyl alcohol with sodium, was chosen as initiator (Scheme 1). This initiator

* Corresponding author. E-mail: sh@chemie.hu-berlin.de.
† Humboldt-Universität zu Berlin.
‡ Max-Planck-Institut für Kohlenforschung.

10.1021/ma702844w CCC: $40.75
Published on Web 04/17/2008

Scheme 1. Synthesis of Isotactic, Nonracemic Poly(propylene oxide)s 2 by Anionic Ring-Opening Polymerization and Activation to Aryl Iodides 4 (a: $n = 100$; b: $n = 200$; c: $n = 400$; d: $n = 40$)

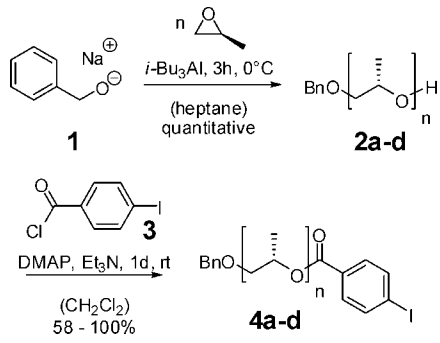

offers several distinct advantages as opposed to metal hydroxides since it yields monofunctional polymers, acts as convenient UV label during work-up and analysis, and can subsequently be removed by hydrogenolysis followed by postfunctionalization, for example with various carboxylic acid derivatives. The catalyst triisobutylaluminum plays a dual role in controlling the growth, since it activates the monomer for an accelerated addition to the propagating chain end by coordination to the PO's oxygen and it inhibits defect formation by lowering the basicity of the active chain end.

The polymerizations were run in heptane−toluene solvent mixtures at 0 °C. The reaction was quenched with acidic ethanol after 3 h, after which time all monomer was consumed. The reaction conditions were optimized for the polymerization of racemic PO in terms of control of chain length and polydispersity, and selected results for atactic and isotactic PPOs **2** are presented in Table 1. An optimal catalyst:initiator ratio of 7:1 was chosen.

Purification and fractionation of atactic PPO ***a*-2** was only possible by precipitation in water−methanol mixtures. Instead, isotactic PPO **2** and all its derivatives could readily be recrystallized from acetone at −20 °C.

Characterization. All PPOs were fully characterized. GPC analysis using polystyrene standards for calibration overestimated the molecular weight; however, chain lengths could conveniently be determined by ^{1}H NMR end-group analysis (Figure 1). The GPC results were used to determine the polydispersity while ^{13}C NMR spectroscopy was employed to monitor tacticity.

For comparison, Figure 2 shows NMR spectra of a representative atactic and isotactic PPOs. While the ^{1}H NMR spectra differ only in the splitting of the methyl signal, the ^{13}C NMR spectra display eye-catching differences. In the spectrum of the atactic polymer, even triads and tetrads consisting of all possible stereosequences were assigned,[11] proving the presence of fully atactic material. This is further supported by the observation that no crystalline (i.e., isotactic) material could be precipitated in cold acetone at all. In contrast, the spectrum of isotactic PPO displays a significantly reduced number of signals, demonstrating the high degree of isotacticity and absence of regioinversion defects.[12]

As PPOs lack UV/vis-active chromophoric groups, optical spectroscopy is limited by solvent absorbance and spectrometer setup. A representative absorbance and CD spectrum for the isotactic and optically active PPO **2b** in acetonitrile is shown in Figure 3. Polyether backbone absorption emerges below 220 nm while transmission in acetonitrile is negligible down to 190 nm. The observed circular dichroism (CD) spectrum is agreement with the literature.[13]

Poly(propylene oxide)−Poly(*p*-phenylene ethynylene) Block Copolymers. *Synthesis.* In order to polymerize phenylene ethynylene monomers onto the PPO, a suitable functional group on the PPO terminus has to be generated. Adequate functionalities for Sonogashira coupling include aromatic iodides and terminal ethynyl groups; however, having the halide function on the starting polymer block prevents incorporation of diyne defects into the growing backbone anchored to the first segment. As the present PPO blocks are all hydroxyl-terminated, an ester moiety was chosen to serve as the linker, and hence 4-iodobenzoic acid was chosen for activating the PPO terminus toward Sonogashira−Hagihara cross-coupling reactions (Scheme 1).

4-Iodobenzoic acid was quantitatively converted to the activated acid chloride **3** and subsequently condensed with the monofunctional PPO blocks **2** of different lengths (Scheme 1). The acid chloride was used in 10-fold excess in combination with prolonged reaction times to ensure complete coverage of all PPO blocks, as access to their reactive hydroxyl sites might be kinetically hindered by partial embedment in PPO coils. After aqueous work-up, the obtained activated PPOs **4** were purified by recrystallization from acetone at −20 °C to remove remaining reagents while final traces of meanwhile hydrolyzed acid chloride were removed by precipitation in cold dichloromethane. All PPOs and their derivatives that had contact with water or protic polar solvents were further purified by azeotropic concentration of benzene solutions and drying of the solids in vacuo. Complete conversion of all hydroxyl groups was confirmed by end-group analysis using ^{1}H NMR. The yield was lowest for the short PPO, probably due to losses in the recrystallization steps.

The obtained iodoaryl-terminated PPO blocks **4** were reacted with a 100-fold excess of phenylene ethynylene monomers **5** or **6** (Scheme 2). This prolonged Sonogashira polycondensation for generation of the second segment provided the desired diblock copolymers **7** and **8**, respectively (Table 2).

The purification of the resulting crude block copolymers turned out to be tedious. PE homopolymers aggregated extensively with aromatic segments of block copolymers forming colloidal suspensions, which proved inseparable by simple purification steps. For ^{1}H NMR determination of PPE block lengths (vide infra) extremely pure block copolymers are required as homo-PPEs and aromatic phosphorus compounds present as impurities display chemical shifts interfering with the PPE block signals. A combination of several purification steps including precipitations, filtrations, recrystallizations, and centrifugations gave noncolloidal material that was further purified by column chromatography on silica gel using eluent gradients to remove short PE oligomers. Finally, repeated recrystallizations from acetone at −20 °C gradually removed aromatic phosphorus compounds (mainly triphenylphosphine oxide) that possessed identical R_f values as PPO and were not removed by column chromatography.

Among the pure block copolymers, changes of the molecular weight as determined by GPC were too small to be useful for reliable calculation of the degrees of polymerizations for the second block, but ^{1}H NMR analysis revealed constant PPE chain lengths of $m = 10-14$ repeating units for all different PPO block lengths. This is attributed to a similar steric hindrance at all reactive PPO-bound sites independent of the propylene oxide chain lengths, which differ considerably and probably point to well-solubilized blocks openly exposed to the solvent. Thus, the short PPE backbone lengths might be due to intrinsic limitations of the polycondensation approach itself. For comparison reasons, a P*p*PE homopolymer was synthesized directly from the *para* monomer.[14] Most of the isolated material was completely insoluble. GPC analysis of the soluble fraction revealed degrees of polymerization of $n = 6-10$. This finding is in agreement with the upper chain length limit for unsubsti-

Table 1. Polymerization Results for Atactic PPOs a-2 Based on Racemic PO and Isotactic PPOs 2 Based on Enantiopure (*S*)-PO

	isotactic, nonracemic PPOs				atactic, racemic PPOs				
	2a	**2b**	**2c**	**2d**	**a-2a**	***a*-2b**	***a*-2b′**	***a*-2b″**	***a*-2c**
M:I ratio	69:1	200:1	333:1	33:1	69:1	196:1	196:1	200:1	400:1
cat:I ratio	7	7	7	5	7	5	7	9	7
M_n (theory)	4100	11 700	19 500	2000	4100	11 500	11 500	11 500	23 300
M_n (GPC)	6500	14 300	50 000	8300	17 000	35 000	32 000	37 000	44 000
M_n (NMR)	5300	12 700	24 700	2900	5000		11 300	14 800	20 800
PDI (M_w:M_n)	1.90	1.16	1.25	1.10	1.17	1.22	1.18	1.18	1.23

tuted soluble P*p*PEs.[15] The length of the aromatic blocks in the block copolymers compared with the amount of equivalents of monomer used revealed that around one-tenth of all monomers coupled to the PPO. The competing reaction of homocoupling between monomers in solution is much more favorable for reasons of monomer accessability and probability of catalyst encounter as well as of number of reactive sites, i.e., two per monomer and one for the macromolecular capper. The homo-oligomers in solution then quickly grow to a critical length at which they precipitate and are removed from the reaction mixture before they statistically encounter a block copolymer to couple with.

Characterization. Figure 4 illustrates the effects of aggregation on GPC traces. An activated PPO strand **4b** with a molecular weight of $M_n \approx 12\,900$ (determined by ^{1}H NMR) is shown in red. The corresponding purified block copolymer **7b** is shown in blue. The bimodal nature of the blue curve arises from aggregation of the block copolymer. The sharp lower molecular weight signal corresponds to the nonaggregated block copolymer and is only slightly shifted as compared to the parent PPO block **4b** because the P*p*PE block contributes only with 1000−1500 mass units to the copolymer. The higher molecular weight signal arises from aggregation of the rodlike segments, and the degree of aggregation is significant considering the intensity and retention time of the band. Aggregation was conveniently proven by dilution experiments, in which the ratio of the intensities of polymer and its aggregate increased with decreasing concentration.[14]

Optical Spectroscopy. Initial spectroscopic studies were performed on the block copolymer **7b** with a medium PPO block length of $M_n \approx 10\,000$. Absorbance spectra of polymer solutions at same concentrations in different solvents are depicted in Figure 5, top. In chloroform, the most intense absorbance was observed probably due to the lowest degree of aggregation of the block copolymer. Here, the absorbance maximum is located at 349 nm. In hexane and methanol, which fail to solvate the aromatic P*p*PE segment and therefore lead to enhanced aggregation, the absorbance maximum displays a hypsochromic shift to 335 nm, and in methanol−water mixtures the maximum is further shifted to 331 nm.

Large differences were observed in the fluorescence spectra. The emission curves of **7b** in several solvents are shown in Figure 5, middle. All signals are essentially bimodal, possessing a peak at lower wavelengths corresponding to nonaggregated P*p*PEs and a peak at longer wavelengths caused by excimer-like emission[16] of aggregated and interacting aromatic units. In chloroform, which solvates both blocks of the copolymer, the blue-shifted signal associated with the nonaggregated P*p*PE is much stronger, while in methanol both peaks have similar intensities and the overall emission intensity is dramatically reduced due to strong fluorescence quenching. Finally, in methanol−water mixtures hardly any fluorescence was detectable, inhibited by strongest tendencies toward aggregation (no reliable ratio determination possible). The emission in hexane is rather remarkable since the shape of the bimodal emission curve resembles the curve in chloroform in terms of peak ratio and overall intensity, but the curve is significantly blue-shifted by 13−16 nm. The peak ratios develop upon concentration changes nearly identical to the changes observed in chloroform. In chloroform, both blocks of the copolymer are well solvated,

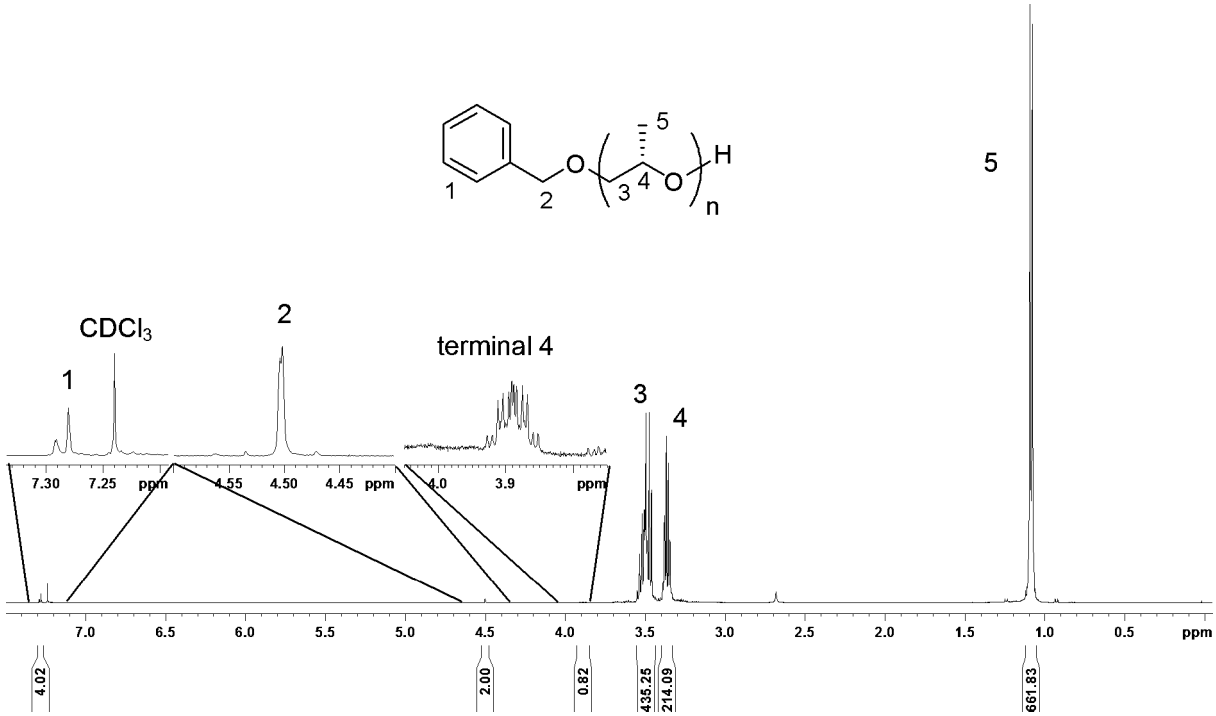

Figure 1. ^{1}H NMR spectrum of PPO **2b** ($CDCl_3$, 23 °C). The ratio of protons H-2:H-3 = 2:435 translates to $M_n \approx 12\,700$.

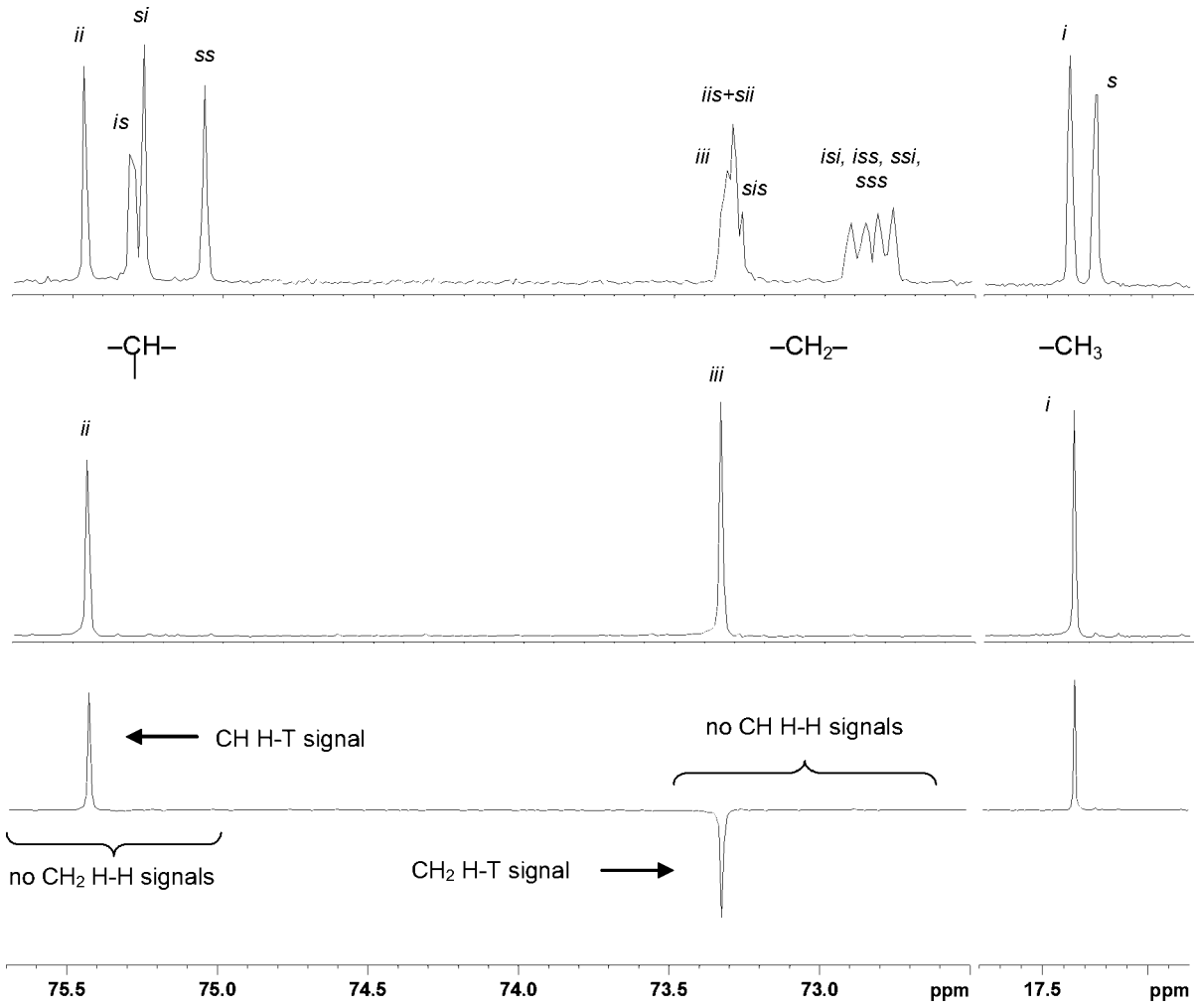

Figure 2. NMR spectra of PPOs ($CDCl_3$, 23 °C): ^{13}C NMR spectrum of atactic ***a*-2b** (top) and isotactic **2b** (middle); 135° DEPT-NMR spectrum of isotactic PPO **2b** (bottom). The indices *i* and *s* refer to isotactic and syndiotactic diads, triads, and tetrads; H−T and H−H refer to head-to-tail and head-to-head connectivity, respectively.

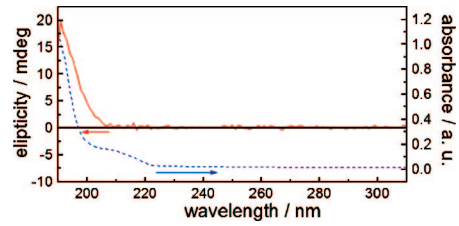

Figure 3. UV/vis absorption (dashed blue) and CD (red) spectra of PPO **2b** (0.19 g/L, in acetonitrile, 20 °C).

thereby limiting aggregation and hence explaining the lack of optical activity; i.e., no CD signal can be detected (Figure 5, bottom). In contrast, optical activity is present in hexane solutions and resembles the activity in methanol. As methanol solvates PPO but not P*p*PE, the block copolymer aggregates with the rigid block, presumably assembling into chiral stacks with the PPO segments being exposed to the solvent and forming the sheath around the stacks keeping the supramolecular structure in solution. As the stacking occurs with a preferred twist sense induced by chirality transfer from the PPO segments, a bisignate CD signal in the transition region of the P*p*PE backbone can be observed. Increasing the effect of amphiphilicity in the copolymer by adding water as cosolvent leads to further fluorescence quenching; however, regarding chirality transfer, the maximum CD signal is already achieved in pure methanol. Hexane resembles a poor solvent for both the P*p*PE

Scheme 2. Polycondensation of 4-Iodophenylacetylene 5 or 3-Iodophenylacetylene 6 in the Presence of Activated PPOs 4 of Different Lengths (a: $n = 100$; b: $n = 200$; c: $n = 400$)

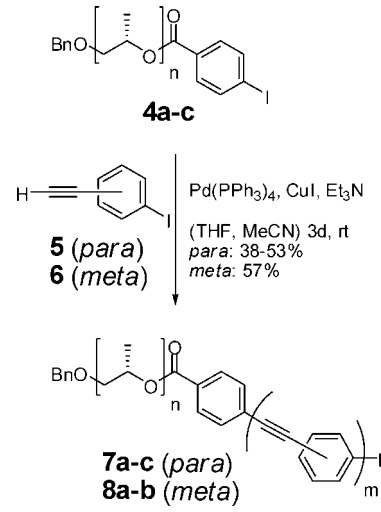

and PPO segments, and therefore the PPO block adopts a more compact coil structure, presumably embedding the rodlike aromatic block. This leads to (i) a change in polarity around the P*p*PE explaining the hypsochromic shift in the absorbance spectra, (ii) an isolation of the P*p*PE blocks from each other

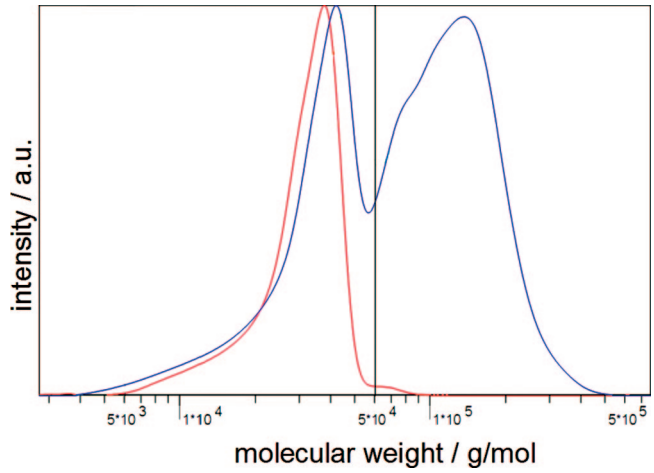

Figure 4. Overlay of GPC traces for activated PPO block **4b** (red) and corresponding PPO−P*p*PE block copolymer **7b** (THF, 40 °C).

Table 2. PPO−PPE Block and Graft Copolymers Synthesized by Polycondensation Routes from Monofunctional PPO Blocks 2 (Table 1)

	7a	7b	7c	a-7	8a	8b	12
M_n (NMR)	6300	16 900	30 500	21 400	9200	14 300	123 000[a]
n_{PPO} (NMR)	84	268	499	357	136	229	207
m_{PPE} (NMR)	12	12	14	5	11	8	9[b]

[a] By analytical ultracentrifugation. [b] By GPC using universal calibration.

leading to enhanced fluorescence emission from nonaggregated species, and (iii) a chiral environment around the P*p*PE backbone accounting for the CD activity in absence of aggregation.

The behavior of the other block copolymers with shorter and longer PPO segments, **7a** and **7c**, respectively, is similar for the different solvents. Overlays of emission spectra in chloroform and methanol for all three block copolymers **7a**−**c** are shown in Figure 6, top, to study the influence of the PPO block length on the aggregation. All spectra were normalized to same intensity for comparison purposes. In chloroform the emission spectra for **7a** and **7b** look more or less the same, while the spectrum for **7c** with the longest PO segment possesses features indicating an increased presence of excimers. In methanol, the shorter the PPO chain length, the less intense develops the signal at longer wavelengths attributed to excimer emission. Apparently, the long PPO segments of **7c** better support the existence of aggregates due to superior solubility and better shielding of the assemblies. The effect of temperature on aggregation is almost negligible.[14]

In Figure 6, bottom, CD spectra of block copolymers of the type PPO-*b*-P*p*PE are shown. In chloroform (left), both block segments of the series **7a**−**c** are well solubilized. Thus, no aggregation occurs and no chirality transfer takes place. Instead, in methanol the aromatic segments aggregate to presumably chiral stacks with a preferred screw sense, thus giving rise to a CD signal at 300−425 nm (Figure 6, bottom right). The tendency to aggregate depends primarily on two factors: the solubilizing power and the bulkiness of the PPO block. The excellent solubilizing power of the longest PPO block in **7c** accounts for a still good solubility of the whole block copolymer in methanol and at the same time complicates stacking of the aromatic segment due to its bulkiness, leading to either less extended or less ordered stacks. Thus, the optical activity is the lowest among the three block copolymers of differing PPO chain lengths. On the other extreme, block copolymer **7a** with the shortest PPO strand displays the strongest optical activity for the same reasons given before, i.e., lower solubilizing power due to reduced PPO chain length and smallest bulkiness to

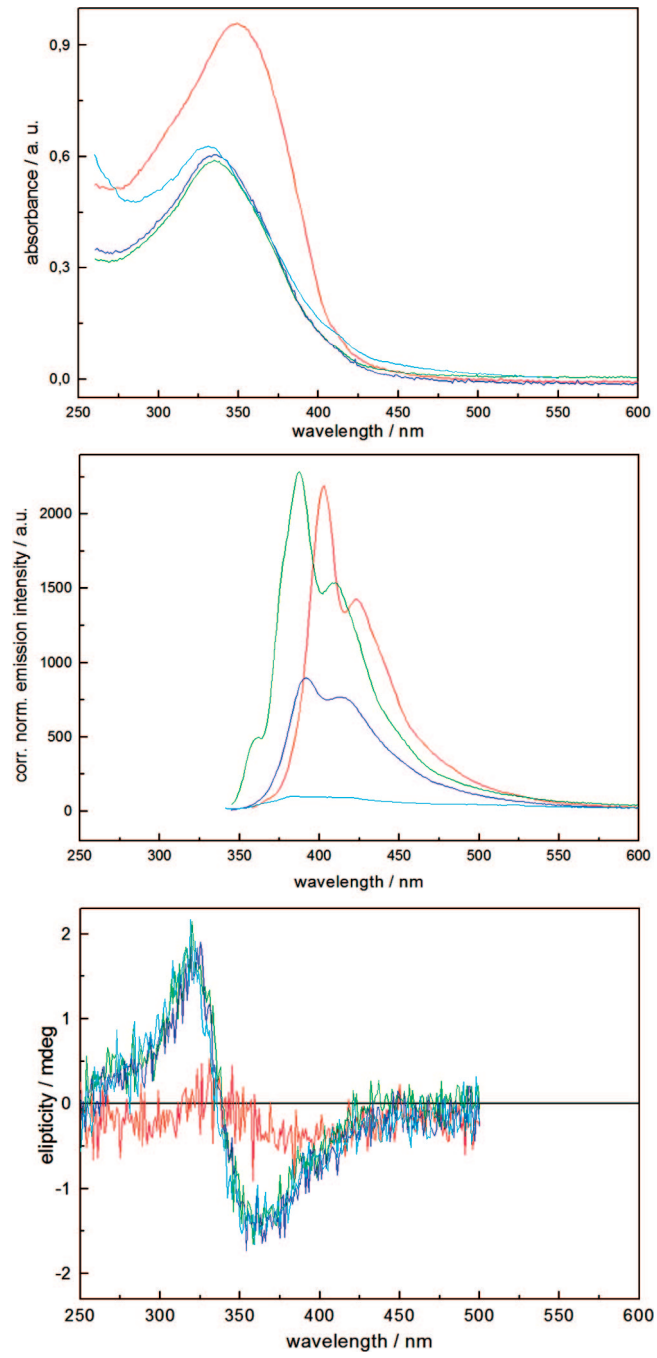

Figure 5. UV/vis absorption (top), emission (middle), and CD (bottom) spectra of block copolymer **7b** in chloroform (red), *n*-hexane (olive), methanol (blue), and methanol−water mixtures (2:1 v/v, cyan) at identical concentrations (91 μg/mL) measured at 25 °C.

thwart stacking propensity. The compilation on the right displays in addition the CD spectrum for block copolymer **a-7**, an analogue of **7b** possessing an atactic PPO block. Both block copolymers generate similar absorbance and emission spectra, but concerning optical activity, no CD signal is observable for **a-7** in methanol, as opposite chiral information is transferred equally to the aromatic P*p*PE block, leading to formation of a racemic mixture with no enantiomeric excess. The absolute values of the CD activity of polymers **7** are moderate only. In contrast to the ideal π,π-stacking distance of planar aromatic systems amounting to ∼3.5 Å, PPO strands adopt a minimal distance of at least 4.7 Å in the close-packed, crystalline solid (shortest edge of unit cell as determined by X-ray analysis).[17] Presumably, this structural incommensurability leads to a less

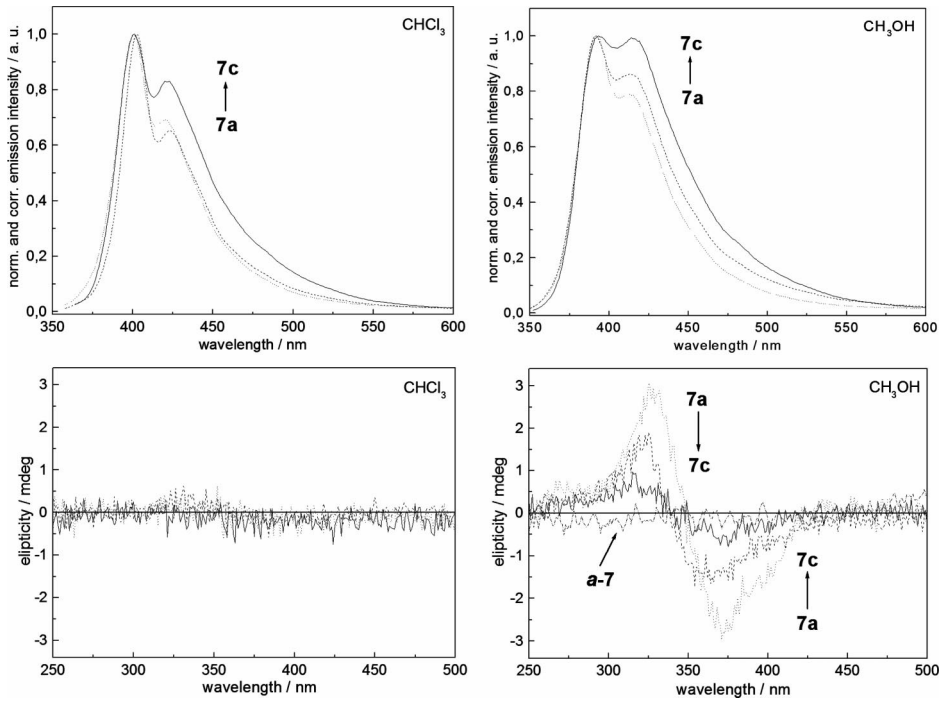

Figure 6. Emission (top) and CD (bottom) spectra of block copolymers **7a** (dotted), **7b** (dashed), and **7c** (solid) in chloroform (left) and methanol (right) measured at 25 °C. Emission spectra have been normalized to the same intensities, and CD spectra include atactic, racemic block copolymer **a-7** for comparison reasons. Concentrations were adjusted to optical densities OD ≈ 0.1 for emission (30, 10, and 8 mg/L in $CHCl_3$ and 13, 19, and 13 mg/L in CH_3OH for **7a**, **7b**, and **7c**) and OD ≈ 1.0 for CD spectroscopy (150, 180, and 130 mg/L in $CHCl_3$ and 130, 220, and 160 mg/L in CH_3OH for **7a**, **7b**, and **7c**).

ordered organization and thus to a rather inefficient chirality transfer.

The changes of absorbance and emission as a function of concentration have been analyzed for all three copolymers in different solvents (Figure 7). The summary of the absorbance data (Figure 7, top) does not reveal unequivocal conclusions. With increasing concentration, absorbance more dramatically increases in chloroform than in methanol due to less pronounced aggregation. Similarly, all copolymers display stronger emission in chloroform than in methanol (Figure 7, bottom). The fluorescence data show that in chloroform copolymer **7a** with the shortest PPO segment displays the least intense emission of all copolymers (although still more intense than any copolymer in methanol), and consequently, in methanol the copolymer **7c** with the longest PPO block displays a lower degree of quenching than the other copolymers with shorter PPO segments.

Poly(propylene oxide)−Poly(*m*-phenylene ethynylene) Block Copolymers. *Synthesis.* The synthetic route to PPO−P*m*PE block copolymers **8** resembles the one for PPO−P*p*PE block copolymers **7**. The same PPO derivatives **2**, activated by esterification with 4-iodobenzoic acid, were each mixed with a 100-fold molar excess of 3-iodophenylacetylene monomer **6** and submitted to Sonogashira−Hagihara polycondensation reactions (Scheme 2). The crude block copolymers were easily generated, but again purification was tedious, as the concurrently produced homopolymer P*m*PE formed stable colloidal complexes with the block copolymer and phosphorus compounds coprecipitated with the block copolymer during the last purification steps. These obstructions dramatically lowered the yields as significant amounts of material were lost along several purification steps. Again, highly pure material was needed to determine the length of the aromatic block by ^{1}H NMR, as GPC differences were too small to be reliable and calibration with polystyrene samples led to incorrect values in this case. Independent of the length of the PPO block, degrees of polymerization for the P*m*PE block were always around $m = 8-11$ repeating units, hence on the verge of being able to fold into stable helices. According to Moore and co-workers, an amphiphilic electron-poor *m*-phenylene ethynylene backbone starts to fold at a chain length of ~10−12 repeat units,[18] and a corresponding less electron-deficient backbone would require more repeating units to adopt a stable helix,[19] as stabilization by aromatic π,π-interactions weaken with increasing electron density in the aromatic rings.[20] In order to increase the length of the rod segment, an alternating approach to block copolymers, i.e., the condensation of a preformed P*m*PE block with the PPO segment, was targeted. For this purpose, monomer **6** was polymerized to the corresponding unsubstituted P*m*PE under various reaction conditions to maximize chain length yet at the same time minimize formation of insoluble high molecular weight polymers, which lower the yield of further utilizable material. However, an approximate average number of repeating units of $n = 15$ only could be achieved, and hence, this route was not followed further.[14] As in the case of PPO−P*p*PE block copolymers (vide supra), no practical benefit from the coupling of these preformed P*m*PE blocks with a PPO segment can be gained as compared to the first approach of directly polymerizing the monomer in the presence of the activated PPO block.

Optical Spectroscopy. The effects of different solvents on the potential helical folding process were determined by monitoring UV absorbances as well as their corresponding absorbance ratios associated with both the folded and random coil states.[18] The absorbance spectra of block copolymer **8b** consist of one band with two pronounced vibrational bands (Figure 8, top). Methanol, which is a poor solvent for the aromatic segment and thus should promote folding, indeed gives lower absorbance ratio values ($abs_{301\ nm}/abs_{285\ nm} = 0.86$) compared to chloroform ($abs_{305\ nm}/abs_{288\ nm} = 0.92$) as described in the literature for related O*m*PEs,[18] consistent with an increasing population of the (partially) folded conformation. The emission in chloroform resembles a narrow intense

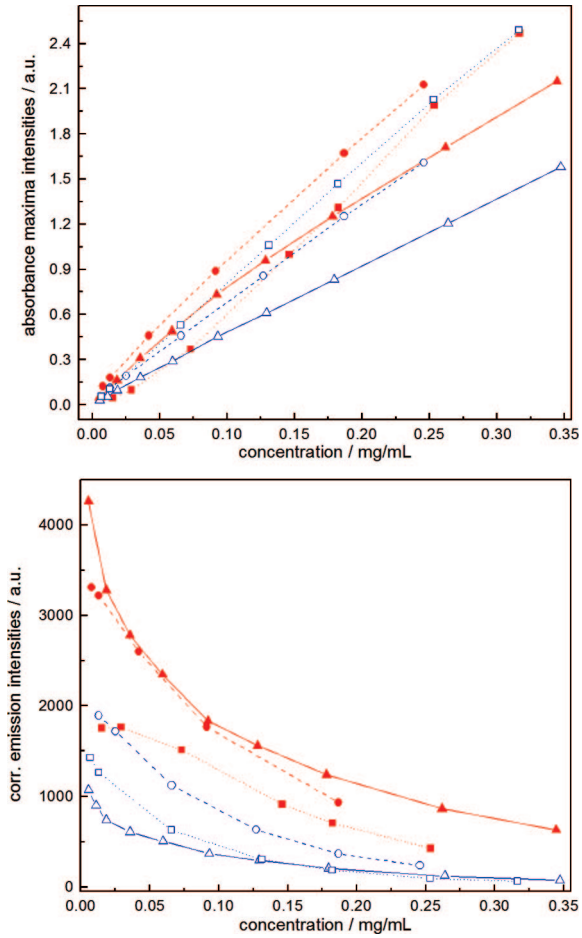

Figure 7. Absorbance maximum intensities (top) and emission intensities (bottom) vs concentration for different block copolymers **7a** (squares), **7b** (triangles), and **7c** (circles) in chloroform (red) and methanol (blue). Connecting lines are included as guide to the eye only.

monomodal signal with little off-tailing, typical for unfolded and nonaggregated *m*-phenylene ethynylenes (Figure 8, middle). In contrast, the emission in methanol is partly quenched due to aromatic interactions, and at the same time, the broad band of $\pi-\pi$ excimer emission is starting to emerge as a second feature above 400 nm, indicating partial folding.

Solvent effects on the CD signal are small. In methanol as well as in chloroform a positive signal in the region of PE backbone absorption is observed (Figure 8, bottom). Note that no bisignate exciton couplet is observed as expected for a helical conformation of similar α-methyl-branched P*m*PE derivatives.[21] Chirality transfer hence occurs in the unfolded and extended, transoid conformation in chloroform, most likely due to a lamellar-type aggregation.[22] As the P*m*PE backbones are very short, no large signal changes are expected—if at all—nevertheless, an increase in ellipticity in methanol is observed. The fraction of longest backbones in the polydisperse P*m*PE segment might fold and give rise to the observed effect. In addition, folding might be enhanced through wrapping of the aromatic backbone by the much larger PPO block, thus encapsulating and stabilizing an otherwise labile (partially) folded PE conformation.

Poly(propylene oxide)−Poly(*m*-phenylene ethynylene) Graft Copolymers. *Synthesis.* The synthesis followed a linear route based on the trifunctional monomer 3-iodo-5-(trimethylsilyl)-ethynylbenzoic acid **9**[21] (Scheme 3). This monomer carried again two orthogonal functional groups for the final Sonogashira polycondensation. First, esterification of the benzoic acid with hydroxyl-terminated poly(propylene oxide) **2b** at room temperature using 1,3-diisopropylcarbodiimide (DIC) and 4-(dimethylamino)pyridinium *p*-toluenesulfonate (DPTS) gave the protected macromonomer **10**. While DIC activates the benzoic acid DPTS has been reported to suppress formation of *N*-acylureas as byproducts.[23] Note that initial esterification attempts using 1-hydroxybenzotriazole (HOBT) and 1-(3′-(dimethylamino)propyl)-3-ethylcarbodiimide (EDC) as standard reagents for amino acid couplings failed to achieve complete coupling. In all esterification reactions, an excess of the benzoic acid component was used to ensure complete coupling at the PPO terminus since remaining unreacted PPO would have been inseparable from the product. The often problematic urea side product was completely removed together with the excess of monomer by repeated precipitations in toluene, in which the macromonomer

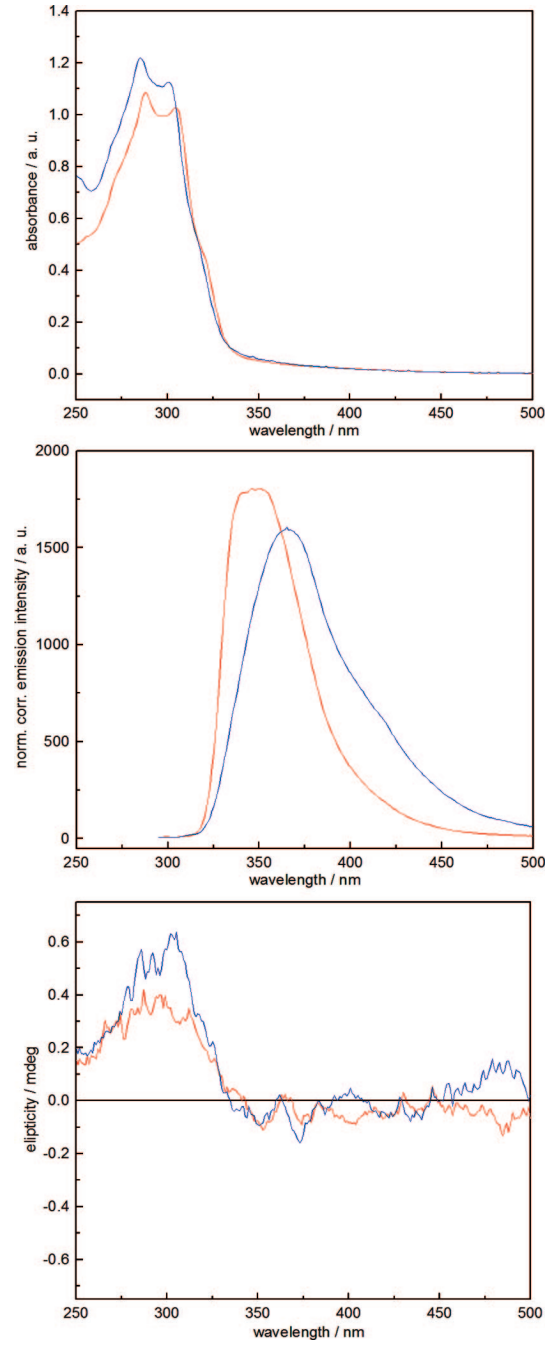

Figure 8. UV/vis absorption (top), emission (middle), and CD (bottom) spectra of block copolymer **8b** in chloroform (red) and methanol (blue) measured at 25 °C. Concentrations were adjusted to optical densities OD ≈ 0.1 for emission (12 mg/L) and OD ≈ 1.0 for UV/vis absorption and CD spectroscopy (125 mg/L).

Scheme 3. Synthesis of PPO-Esterified Unprotected Macromonomer 11 and Its Sonogashira−Hagihara Polycondensation to Graft Copolymer 12 (2b: $n = 200$)

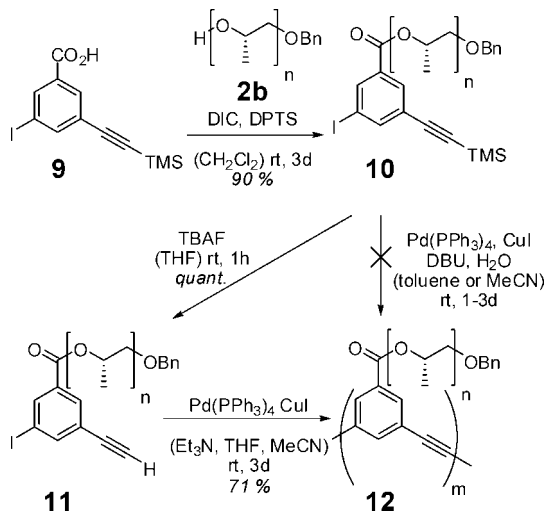

showed good solubility. Surprisingly, direct Sonogashira polycondensation of macromonomer **10** applying the in-situ acetylene deprotection protocol was unsatisfactory. Under these polymerization conditions including the use of base and water, partial saponification of the benzoate was observed by GPC in all attempts and could not be prevented by optimizing reaction conditions. Surprisingly, in several examples using our in-situ deprotection polycondensation protocol[21,24] no signs of saponification have been detected when monomers carrying more polar oligo(ethylene glycol)-based side chains attached via ester bonds were polymerized. Thus, polycondensation conditions had to be adjusted, and the trimethylsilyl group was removed in an extra reaction step using tetra-*n*-butylammonium fluoride (TBAF), allowing the reaction to proceed for a relative long time of 1 h to ensure full deprotection of the embedded reactive site. Subsequently, polycondensation of isolated **11** under standard and water-free conditions gave the desired graft copolymer **12** without any detectable saponification. The absolute molecular weight of the resulting graft copolymer **12** was determined via GPC coupled to viscosity (universal calibration) as M_n = 110 000 and M_w = 201 000, respectively. Independently, determination of molecular weight by ultracentrifugation gave similar values (M_w = 240 000). Since the molecular weight of the macromonomer **11** was reliably determined by ^{1}H NMR end-group analysis as M_n = 12 000, the average number degree of polymerization amounts to approximately $n = 9-10$. Note that NMR end-group analysis cannot be applied in the case of graft copolymers prepared via the macromonomer route.

Spectroscopy. The results from optical spectroscopy are shown in Figure 9. The absorbance spectra in different solvents are very similar, possessing the same features in comparable intensities. Among *m*-phenylene ethynylenes, folding is monitored by a decrease of the shoulder at 300 nm when the good solvent chloroform is replaced by more polar solvents such acetonitrile or methanol. This was only observed after adding water as a cosolvent. Similarly, the fluorescence curves differ in shape around their maxima but possess comparable intensities. The reason for the increased emission intensity in acetonitrile or methanol as compared to chloroform remains ambiguous. Again, water addition was necessary to observe (partial) quenching of the emission arising from the cross-conjugated monomer units and subsequent broadening together with a new shoulder above 400 nm, which can be attributed to excimer formation among adjacent aromatic backbones. An overlay of the CD spectra illustrates the solvent-driven induction of optical

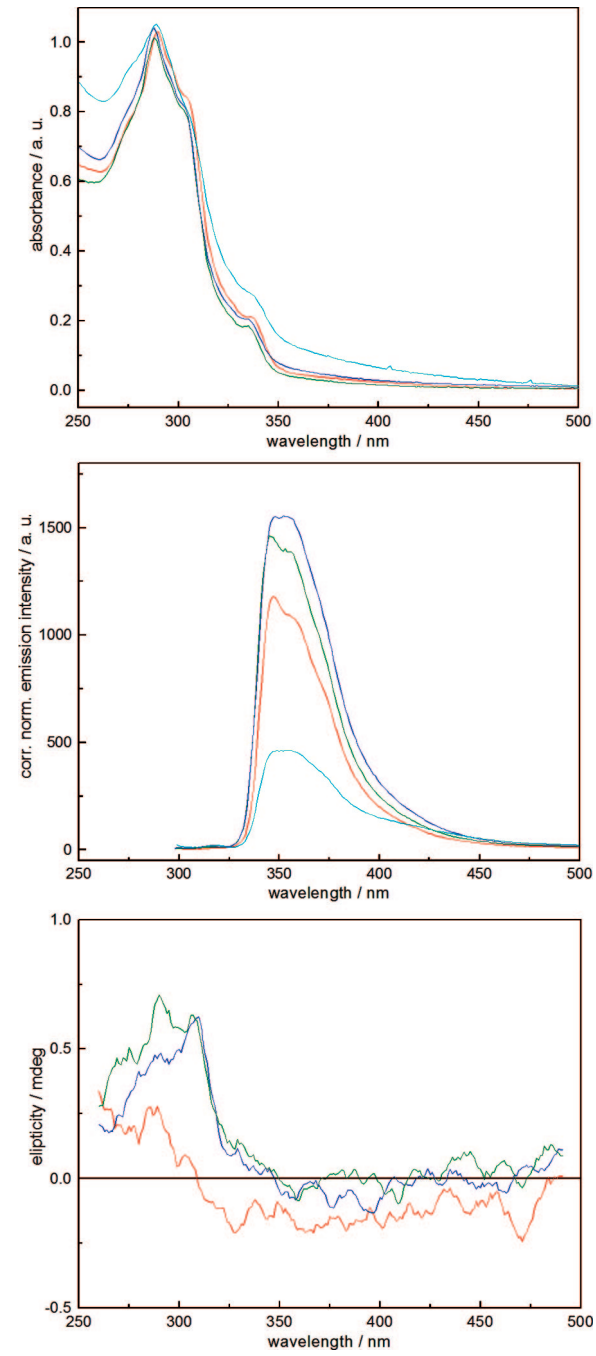

Figure 9. UV/vis absorption (top), emission (middle), and CD (bottom) spectra of graft copolymer **12** in chloroform (red), acetonitrile (olive), methanol (blue), and methanol−water mixture (2:1 v/v, cyan) measured at 25 °C. Concentrations were adjusted to optical densities OD ≈ 0.1 for emission (40 mg/L) and OD ≈ 1.0 for UV/vis absorption and CD spectroscopy (400 mg/L).

activity (Figure 9, bottom). In chloroform a minor activity is observed, as the aromatic backbone probably adopts an extended conformation in order to minimize steric repulsion of the bulky PPO side chains. In polar solvents, such as acetonitrile or methanol, an increase of optical activity is observed, attributed to the helical folding of the backbone, which retreats from the solvent. The moderate effect might be explained by either an inefficient chirality transfer from the PPO chains to the aromatic backbone or a hindered folding. To attain a stable helix with favorable aromatic π,π-interactions between turns, a pitch of 3.4 Å has to be attained, while nonracemic PPO pack in the bulk with minimal distances of 4.7 Å (vide supra),[17] thus conflicting with the folding event. The PPO chains with a

number average molecular weight of M_n = 10 000 g/mol corresponding to ~200 repeating unit are very long and numerous compared to the dimensions of a helical turn and therefore contribute substantial bulkiness to the system. While a helical backbone possesses an outer diameter of 20 Å, the extended PPO chains spread across over 700 Å in their packed conformation.[17] As PPO chains are attached to every repeating unit of the backbone, significant steric constrains are generated and limit the conformational freedom and the P*m*PE backbone's tendency to fold. Stacking of short helices would further stabilize this conformation but should again be aggravated by the bulkiness of PPO side chains wrapping the aromatic backbone.

Summary

Successful construction of a series of amphiphilic block copolymers based on a flexible nonracemic PPO segment and an aromatic PE segment was achieved. The PPO segment was polymerized from enantiopure PO, and optimization of reaction conditions yielded highly isotactic, nonracemic, and thus optically active polymeric material of controlled length and low polydispersity. *p*-PE and *m*-PE monomers were successfully polymerized in the presence of the monofunctional PPO segments of different lengths generating block copolymers of distinct architectures, i.e., rod−coil copolymers with π-conjugated aromatic blocks in the case of P*p*PE and switchable segments of differing aspect ratios in the case of P*m*PE undergoing helix−coil transitions. The influence of the connectivity among the aromatic segments as well as the influence of the length of the PPO segment on the block copolymers' solution properties was analyzed by optical spectroscopy studies. Furthermore, the architectural modification of attaching PPO segments on trifunctional PE monomers and their subsequent polymerization lead to graft copolymers of respectable molecular weight. Spectroscopic characterization demonstrated the ability of the P*m*PE backbone to fold although due to the large steric demand of the long PPO side chains water as strong polar cosolvent was needed to overcome the activation barrier of folding based on the hydrophobic effect. Here, shorter PPO segments should facilitate the helix−coil transition while maintaining the advantages of such hybrid macromolecular materials.

The present study outlines a new conceptual approach to integrate chirality into rod−coil block copolymers and graft copolymers via the incorporation of nonracemic PPO side chains. Ongoing work focuses on in depth structural analysis of the present copolymers in the bulk and at interfaces as well as the synthesis of new copolymers incorporating different optoelectronically active components. The use of flexible, enantiomerically pure, PPO segments with orthogonal end-group functionality and narrow dispersity should prove viable for the preparation of new polymer architectures, in which hierarchical structure formation as a consequence of conformational ordering and self-assembly will result in advanced materials properties.

Acknowledgment. The authors are grateful to Christian Kaiser for synthesizing compound **9** and to Helmut Cölfen (MPI for Colloids and Interfaces, Potsdam) for carrying out analytical ultracentrifugation on the polymer brushes. Klaus Hausschild (MPI Mülheim an der Ruhr) is acknowledged for some GPC measurements. M.A.B.B. is indebted to the Studienstiftung des deutschen Volkes for providing a doctoral fellowship.

Supporting Information Available: Experimental details and chemical characterization data. This material is available free of charge via the Internet at http://pubs.acs.org.

References and Notes

(1) For a key review, see: Bates, F. S. *Science* **1991**, *251*, 898–905.
(2) For representative overviews see: (a) Bucknall, D. G.; Anderson, H. L. *Science* **2003**, *302*, 1904–1905. (b) Lee, M.; Cho, B.-K.; Zin, W.-C. *Chem. Rev.* **2001**, *101*, 3869–3892. (c) Klok, H.-A.; Lecommandoux, S. *Adv. Mater.* **2001**, *13*, 1217–1229. (d) Muthukumar, M.; Ober, C. K.; Thomas, E. L. *Science* **1997**, *277*, 1225–1232.
(3) Important examples include: (a) Thurn-Albrecht, T.; Schotter, J.; Kästle, G. A.; Emley, N.; Shibauchi, T.; Krusin-Elbaum, L.; Guarini, K.; Black, C. T.; Tuominen, M. T.; Russell, T. P. *Science* **2000**, *290*, 2126–2129. (b) Thurn-Albrecht, T.; Steiner, R.; DeRouchey, J.; Stafford, C. M.; Huang, E.; Bal, M.; Tuominen, M.; Hawker, C. J.; Russell, T. P. *Adv. Mater.* **2000**, *12*, 787–791. (c) Kim, H.-C.; Jia, X.; Stafford, C. M.; Kim, D. H.; McCarthy, T. J.; Tuominen, M.; Hawker, C. J.; Russell, T. P. *Adv. Mater.* **2001**, *13*, 795–797.
(4) Some selected examples are given in: (a) Leclere, P.; Calderone, A.; Marsitzky, D.; Francke, V.; Geerts, Y.; Müllen, K.; Bredas, J.-L.; Lazzaroni, R. *Adv. Mater.* **2000**, *12*, 1042–1046. (b) Kong, X.; Jenekhe, S. A. *Macromolecules* **2004**, *37*, 8180–8183. (c) Messmore, B. M.; Hulvat, J. F.; Sone, E. D.; Stupp, S. I. *J. Am. Chem. Soc.* **2004**, *126*, 14452–14458. (d) Jahnke, E.; Lieberwirth, I.; Severin, N.; Rabe, J. P.; Frauenrath, H. *Angew. Chem., Int. Ed.* **2006**, *45*, 5383–5386.
(5) Chiral rod segments, namely α-helical polypeptides, have been used (see for example ref 4b), yet chiral flexible coil segments have not been investigated thus far.
(6) A comprehensive review is given in: Hoeben, F. J. M.; Jonkheijm, P.; Meijer, E. W.; Schenning, A. P. H. J. *Chem. Rev.* **2005**, *105*, 1491–1546.
(7) A comprehensive review is provided by: Yashima, E.; Maeda, K. In *Foldamers: Structure, Properties, and Applications*; Hecht, S., Huc, I., Eds.; Wiley-VCH: Weinheim, 2007; pp 331−336.
(8) Please note that due to the polycondensation mechanism, a clear distinction of "graft from" and "attach to" routes cannot be made in this case.
(9) For a recent review consult: Dickerson, T. J.; Reed, N. N.; Janda, K. D. *Chem. Rev.* **2002**, *102*, 3325–3343.
(10) Billouard, C.; Carlotti, S.; Desbois, P.; Deffieux, A. *Macromolecules* **2004**, *37*, 4038–4043.
(11) Chisholm, M. H.; Navarro-Llobet, D. *Macromolecules* **2002**, *35*, 2389–2392.
(12) Antelmann, B.; Chisholm, M. H.; Iyer, S. S.; Huffman, J. C.; Navarro-Llobet, D.; Pagel, M.; Simonsick, W. J.; Zhong, W. *Macromolecules* **2001**, *34*, 3159–3175.
(13) Hirano, T.; Sato, A.; Tsuruta, T.; Johnson, W. C., Jr. *J. Polym. Sci., Polym. Phys.* **1979**, *17*, 1601–1609.
(14) See Supporting Informationfor details.
(15) (a) Bochmann, M.; Kelly, K. *J. Polym. Sci., Part A: Polym. Chem.* **1992**, *30*, 2503–2510. (b) Lavastre, O.; Ollivier, L.; Dixneuf, P. H.; Sibandhit, S. *Tetrahedron* **1996**, *52*, 5495–5504. (c) Pelter, A.; Jones, D. E. *J. Chem. Soc., Perkin Trans. 1* **2000**, 2289–2294.
(16) More correctly, emission results from a pseudo-excimer as aggregation leads to face-to-face preorganization of the interacting aromatic moieties prior to excitation.
(17) (a) Cesari, M.; Perego, G.; Marconi, W. *Makromol. Chem.* **1966**, *94*, 194–204. (b) Stanley, E.; Litt, M. *J. Polym. Sci.* **1960**, *43*, 453–8.
(18) (a) Nelson, J. C.; Saven, J. G.; Moore, J. S.; Wolynes, P. G. *Science* **1997**, *277*, 1793–1796. (b) Prince, R. B.; Saven, J. G.; Wolynes, P. G.; Moore, J. S. *J. Am. Chem. Soc.* **1999**, *121*, 3114–3121. An account is given in: (c) Stone, M. T.; Heemstra, J. M.; Moore, J. S. *Acc. Chem. Res.* **2006**, *39*, 11–20.
(19) Lahiri, S.; Thompson, J. L.; Moore, J. S. *J. Am. Chem. Soc.* **2000**, *122*, 11315–11319.
(20) For comprehensive reviews on π,π-interactions consult: (a) Hunter, C. A.; Lawson, K. R.; Perkins, J.; Urch, C. J. *J. Chem. Soc., Perkin Trans. 2* **2001**, 651–669. (b) Meyer, E. A.; Castellano, R. K.; Diederich, F. *Angew. Chem., Int. Ed.* **2003**, *42*, 1210–1250.
(21) Kaiser, C. Ph.D. Thesis, Freie Universität Berlin, Germany, **2006**.
(22) (a) Lamellar type aggregation has been observed for *m*-phenylene ethynylene oligomers in the solid state: Prest, P.-J.; Prince, R. B.; Moore, J. S. *J. Am. Chem. Soc.* **1999**, *121*, 5933–5939. (b) Mio, M. J.; Prince, R. B.; Moore, J. S.; Kübel, C.; Martin, D. C. *J. Am. Chem. Soc.* **2000**, *122*, 61346135 79. (c) Kübel, C.; Mio, M. J.; Moore, J. S.; Martin, D. C. *J. Am. Chem. Soc.* **2002**, *124*, 8605–8610.
(23) Moore, J.; Stupp, S. *Macromolecules* **1990**, *23*, 65–70.
(24) (a) Hecht, S.; Khan, A. *Angew. Chem.* **2003**, *42*, 6021–6024. (b) Khan, A.; Hecht, S. *Chem. Commun.* **2004**, 300–301. (c) Khan, A.; Hecht, S. *Synth. Met.* **2004**, *147*, 37–42. (d) Khan, A.; Hecht, S. *J. Polym. Sci., Part A: Polym. Chem.* **2006**, *44*, 1619–1627.

MA702844W